HOKKAIDO UNIVERSITY

Title	Comparison of equatorial wave activity in the tropical tropopause layer and stratosphere represented in reanalyses
Author(s)	Kim, Young-Ha; Kiladis, George N.; Albers, John R. et al.
Citation	Atmospheric Chemistry and Physics, 19(15), 10027-10050 https://doi.org/10.5194/acp-19-10027-2019
Issue Date	2019
Doc URL	https://hdl.handle.net/2115/76284
Rights(URL)	https://creativecommons.org/licenses/by/4.0/
Type	journal article
File Information	acp-19-10027-2019-supplement.pdf

Hokkaido University Collection of Scholarly and Academic Papers : HUSCAP

Supplement of Atmos. Chem. Phys., 19, 10027–10050, 2019
https://doi.org/10.5194/acp-19-10027-2019-supplement
© Author(s) 2019. This work is distributed under
the Creative Commons Attribution 4.0 License.

Atmospheric Chemistry and Physics
Open Access
EGU

Supplement of

Comparison of equatorial wave activity in the tropical tropopause layer and stratosphere represented in reanalyses

Young-Ha Kim et al.

Correspondence to: Young-Ha Kim (kim@iau.uni-frankfurt.de), Changhyun Yoo (cyoo@ewha.ac.kr)

The copyright of individual parts of the supplement might differ from the CC BY 4.0 License.

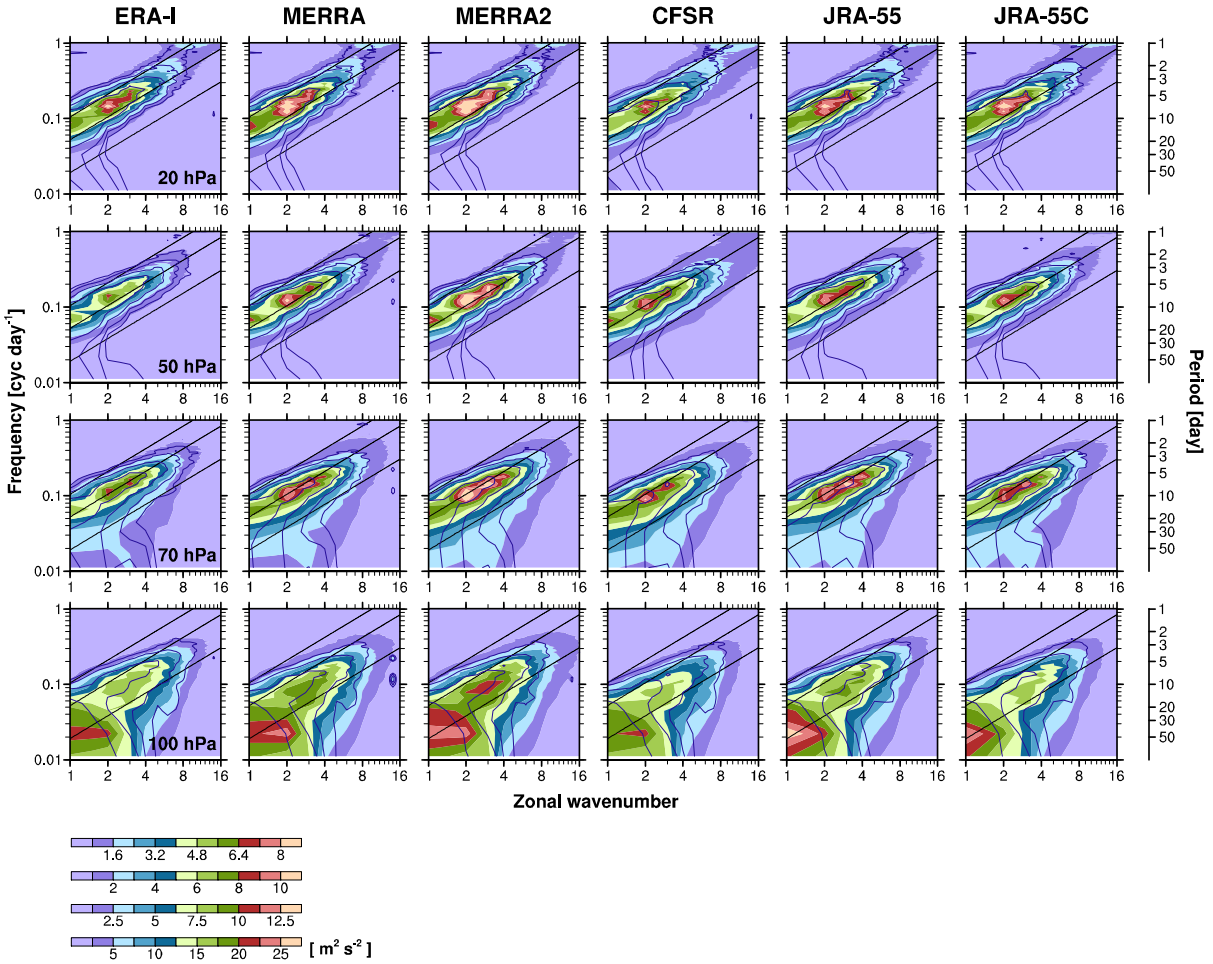


Figure S1. The same as in Fig. 1 except for the zonal wind.

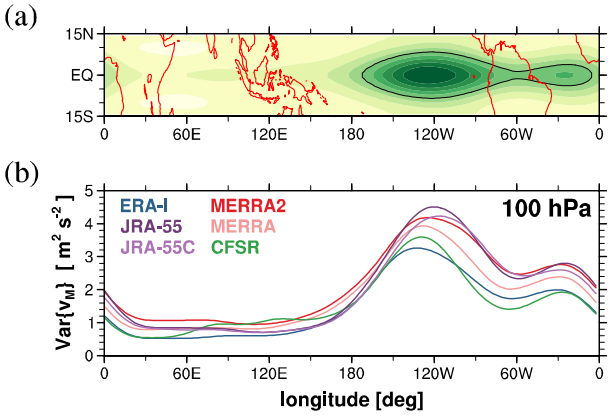


Figure S2. The same as in Fig. 3 except for the 100-hPa symmetric meridional wind filtered for $-10 \leq k < 0$ and $0.033 \leq \omega < 0.1\,\mathrm{cyc\,day^{-1}}$.

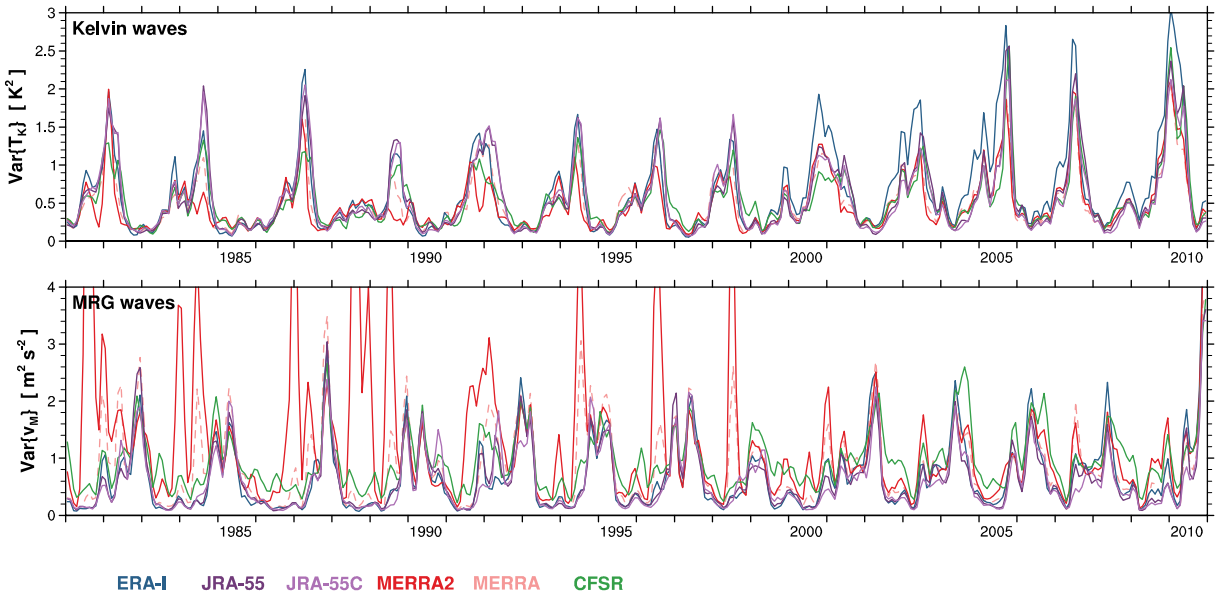


Figure S3. Monthly time series of variances of (upper) temperature for the Kelvin waves (T_{Kelvin}) and (lower) meridional wind for the MRG waves (v_{MRG}) at 10 hPa averaged over 15°N–15°S. The MERRA results are from the standard-level datasets (dashed), and the others from the model-level datasets (solid). See the text in Section 3.1 for the definitions of T_{Kelvin} and v_{MRG}.

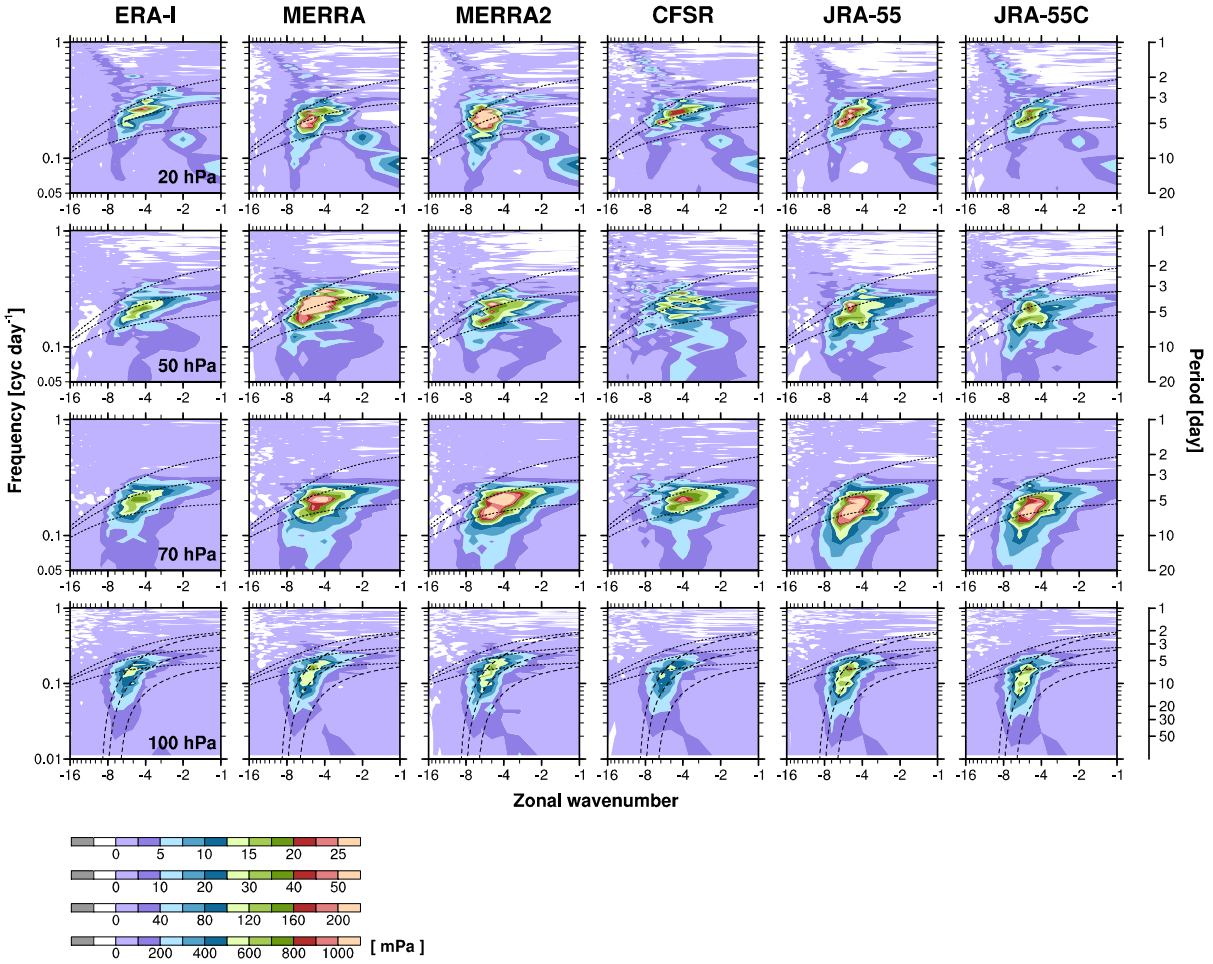


Figure S4. The same as in Fig. 10 except for $\langle F_\phi \rangle$ of antisymmetric modes over 5°N–5°S, where $\langle F_\phi \rangle$ is the latitudinal average of the equatorward EP flux, $\mathrm{sgn}(-\phi)F_\phi$, and ϕ the latitude.

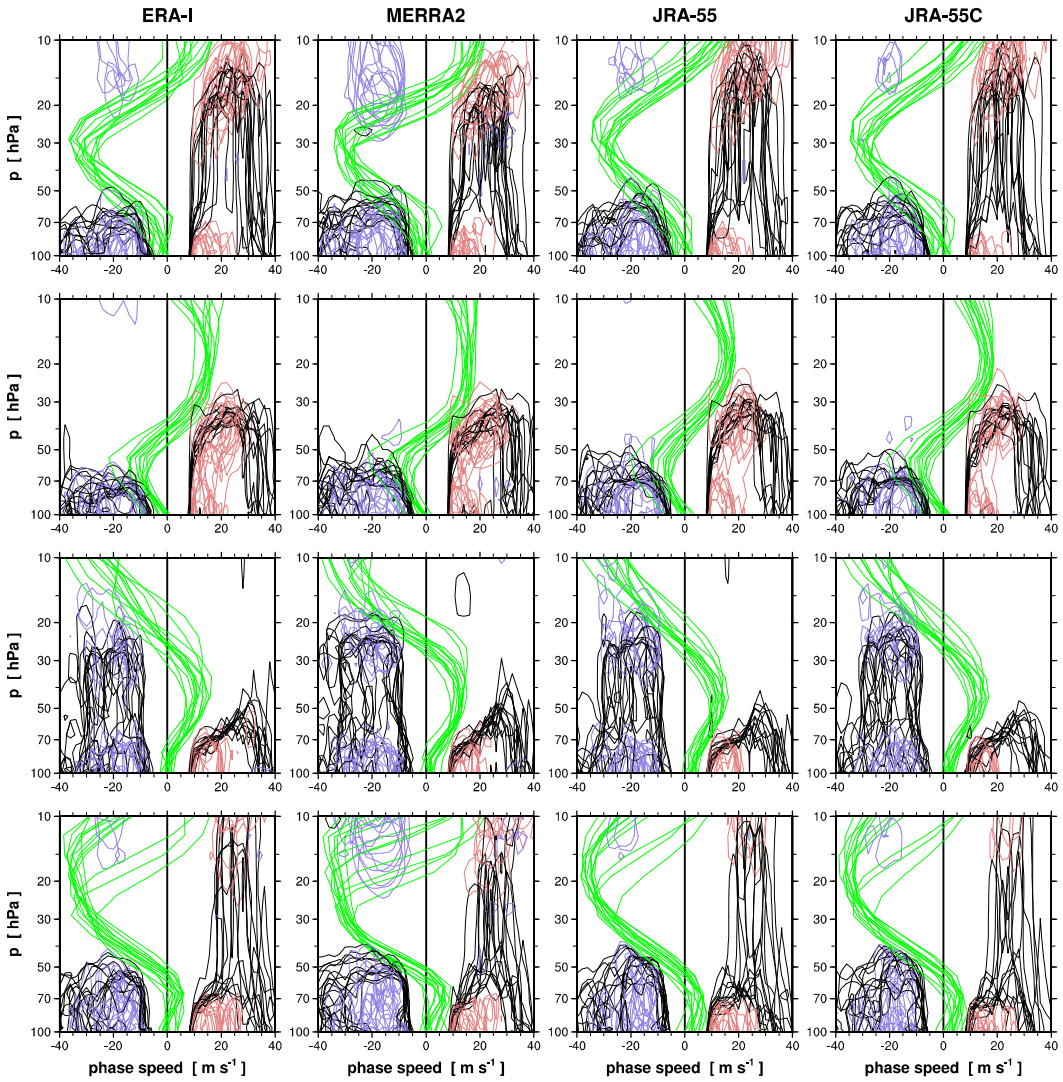


Figure S5. Spaghetti plots for 13 individual QBO cycles within the period of 1981–2010: contours for the Kelvin wave EP flux divergence of $0.3\,\mathrm{m\,s^{-1}\,month^{-1}/(m\,s^{-1})}$ (red), for the MRG wave EP flux divergence of $-0.06\,\mathrm{m\,s^{-1}\,month^{-1}/(m\,s^{-1})}$ (blue), and for the Kelvin and MRG wave F_z (black) of -0.008 and $0.0003\,\mathrm{mPa/(m\,s^{-1})}$, respectively, as a function of phase speed, during the four QBO phases shown in Fig. 11. The zonal-mean zonal-wind profiles are also plotted (green).